PRECISE POSITIONNING OF UNIT CELLS AND EMBEDDED INSTRUMENTATION FOR FABRICATION AND PRESSURE TESTING OF FILAMENT WOUND TUBES

Hilario Hernandez Moreno[1], Bernard Douchin[1], Francis Collombet[1], Peter Davies[2]

1: Laboratoire de Génie Mécanique de Toulouse, PRO²COM, IUT Paul Sabatier,
133 avenue de Rangueil, F 31077 Toulouse CEDEX 4.
2: IFREMER Materials & Structures group, Brest Centre, BP70, F 29280 Plouzané.

ABSTRACT

To analyse the influence of filament winding patterns on the mechanical behaviour and pressure testing of composite tubes, it is necessary to know the exact position of the winding pattern in order to analyse the fabrication process and the initial material condition. In this paper a winding strategy is presented which allows the winding pattern unit cells to be coincident, and an embedded sensor instrumentation system for monitoring filament winding specimens during the different fabrication and testing phases is described.

1. INTRODUCTION

Filament wound tubes have a multi-layer structure with ondulation zones, due to the fabrication process. These ondulation zones form repetitive structures on a mesoscopic level, each one called a unit cell [1]. The normal design methods for these pipes are based on classical laminate theory [2], without considering the heterogeneity inside the unit cell. This heterogeneity may have an influence on the mechanical behaviour if the unit cell dimensions are large compared with the pipe diameter. Some previous papers have looked at the influence of the unit cell in composite filament wound pipes [3-5]. In [3] the weaving influence on mechanical behaviour of thick pipes in torsion was studied. In [4] the influence of interweaving in this kind of structure was studied and in [5] internal pressure tests were performed on pipes. Textile composites have been the focus of a number of studies [6-8] but filament wound pipes under external pressure (which is the primary loading for underwater applications) have not been studied considering this approach.

The first step is to know the initial material condition. This involves knowing the position of each unit cell, and placing them coincident one over the other along the tube. The second step is to monitor the fabrication process. Many studies have examined the health monitoring of composite structures [9-12], and some of these looked at the installation of embedded optical sensors for monitoring the material state of filament wound pipes [12]. In this study embedded sensors are used in order to monitor the response of filament wound specimens, specifically Bragg gratings and thermocouples. These measurement instruments are designed for static operation, so a special interface has been designed between the static and rotary segments. The instrumentation enables internal strains to be measured during fabrication but the same sensors also allow strains in the pipe to be measured during external pressure testing at the IFREMER hydrostatic pressure test facility.

This paper will present the winding strategy used to locate the unit cells accurately and the embedded instrumentation employed to monitor both the specimen fabrication process and subsequent pressure testing.

2. UNIT CELL PRECISE POSITIONING PROGRAM MODIFICATION

The specimens are glass/epoxy composite pipes, with a constant winding angle ($\alpha \pm 55°$), for 5 mm (7 plies) and 15 mm (10 plies) thickness. The fabrication process has two phases: winding and oven curing (see Fig. 1). The winding phase is developed using the three axes numerical

control machine-tool illustrated in Fig. 1a. The working mandrel is attached to the machine spindle.

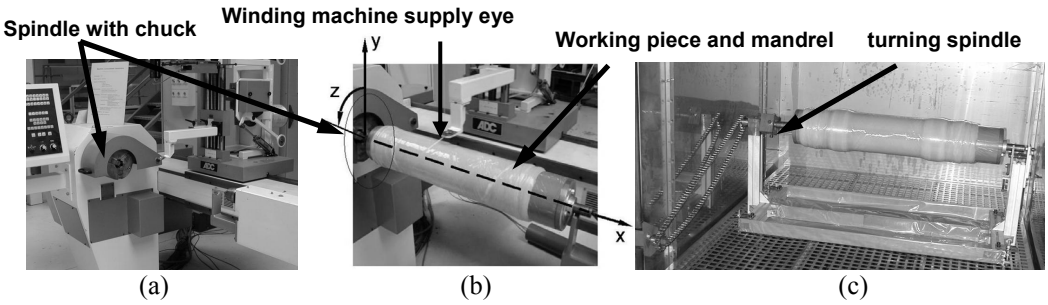

Fig. 1. Filament winding three axes numerical control machine-tool (a), machine axes: *x* axis, longitudinal, *y* axis, vertical, *z* axis, rotation (b), curing configuration (c).

For pipe fabrication, a series of programs have already been written, but unit cell positions were randomly oriented between plies. A kinematic-geometrical analysis revealed the necessity to modify them.

2.1 Classical winding strategy

First, two mandrel revolutions are commanded ($\Delta z = 80$ points[1]). Next, all the rest of the code is in an *S* times cycle loop (*S* is the number of roving positions to completely cover the entire circumference), each cycle is the formation of a branch (going – returning), each going phase is formed by three parts: 1) a transition from 90° to 55° winding angle (short helical displacements), 2) main helical displacement of a 55° winding angle and 3) a transition from 55° to 90° winding angle. The returning segment is completely symmetric to the going one. There is an intermediate rotation between both segments, and a rotation at the end of the returning segment (see Fig. 2). The going-returning path until a roving is placed beside the first one is known as a trajectory. For this particular case there are two kinds of trajectories (one and five unit cell).

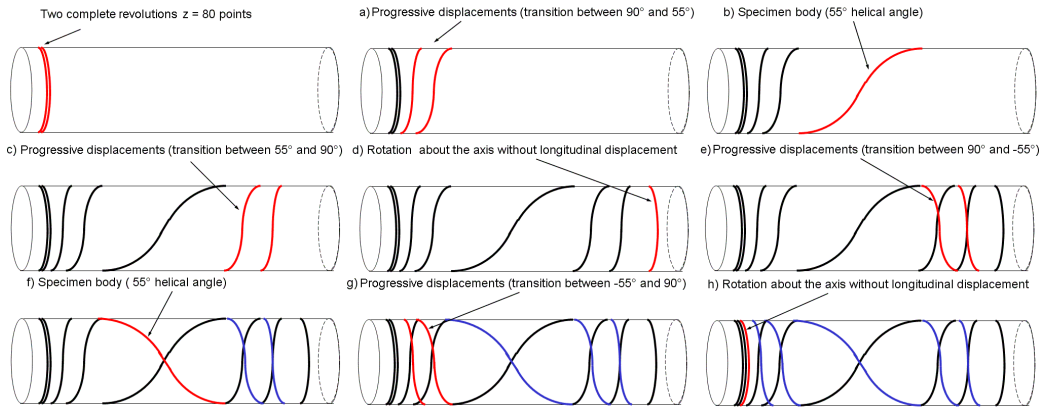

Fig. 2. Branches formation principal segments.

[1] Displacements over the *z* are introduced in terms of points each point is equivalent to $(2\pi/40)$rad , one revolution is equivalent to 40 points.

For a one unit cell trajectory, the addition of all rotations in a cycle must be an integer plus a small rotation equivalent to the tangent pitch.

$$z_t = \sum \Delta z = \frac{40}{S} + (n40) \tag{1}$$

Where z_t is the total displacement within a cycle, Δz is the individual displacement commanded in each code line, S is the number of roving positions needed to completely cover the circumference, n is an integer number of revolutions. For a five unit cell program, it is first necessary to form each branch, the necessary condition is:

$$z_t = (n40) + \frac{40}{B} + \frac{z_{pt}}{B} \quad \text{with} \quad z_{pt} = \frac{40}{S} \tag{2}$$

Where total rotation displacement z_t must be an integer number of revolutions n, plus the rotation corresponding to one branch, plus the rotation equivalent to a tangent pitch z_{pt} over the number of branches B. At the end of the five branches (complete trajectory), the angular rotation is a multiple of 40 plus a rotation equivalent to a tangent pitch ($\Delta z = 40n + z_{pt}$) (see Fig. 3), these conditions are necessary to have a closed trajectory.

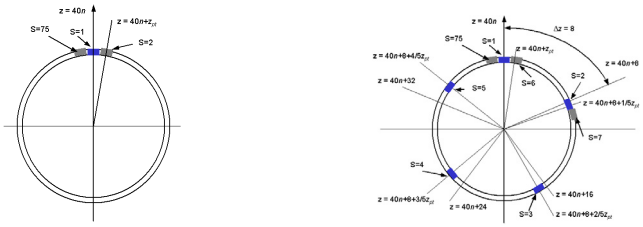

(a) (b)

Fig. 3. Branches formation, (a) one unit cell trajectory, (b) five unit cell trajectory.

2.2 Program modification

First, the crossing point coordinates between going and returning displacements are established (see Fig. 4). Next, find the new crossing point to place the unit cell in the middle of pipe length (see Fig. 4b), and the necessary x displacement. To produce the required Δx displacement it is necessary to rotate the returning path about the z axis (see Fig. 4c), i.e. a z rotation before the returning path begins. The magnitude of Δz is given by Eq. (3).

$$\Delta z = \left[2\frac{z_t}{c_t} tg\alpha \right] \Delta x \tag{3}$$

If the required Δx displacement is positive, the Δz rotation must be positive also, α is the winding angle, c_t the outer circumference and z_t is the rotation corresponding to a complete revolution (see Fig. 4c). At the moment of changing the commanded z displacement, the closed trajectory condition is no longer accomplished, a new z rotation is then necessary to re-establish it. For the one unit cell trajectory program, the new value has been calculated using Eq. (1). For the five unit cell trajectory a new closed trajectory condition was established and also a modification in the winding strategy was introduced.

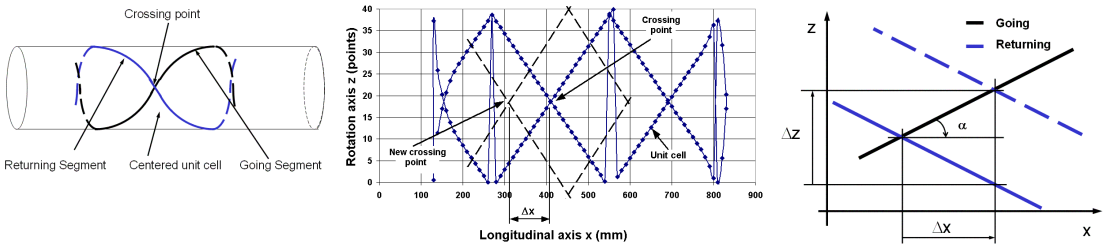

Fig. 4. Crossing point (a), new crossing point position, (b) Δx displacement needed, (c) Relationship between Δx needed and Δz.

In the classical five unit cell strategy, the unit cells did not have the same dimensions, and there was a geometrically theoretical clearance between the last going-returning path of the last unit cell and the first going-returning path of the first unit cell (see Fig. 3b), because the actual roving positions were not placed in the theoretical ones. A new winding strategy has been established to accomplish the closed trajectory condition as a uniform roving distribution. A loop cycle has been added inside the existing loop, the number of cycles within the previous loop has been reduced to accomplish the following condition:

$$S = N_R B \tag{4}$$

Eq. (4) means that it is necessary to repeat N_R times the B number of unit cell trajectory (B branches). The new closed trajectory condition to be accomplished on a B unit cell program is presented in Eq. (5). For a five unit cell program B = 5.

$$z_t = (n40) + \frac{40}{B} \tag{5}$$

Between the main and inner loops, a line has been added for executing a z_{pt} rotation that is equivalent to one tangent pitch. With this new strategy, and the closed trajectory condition stated in Eq. (5), the roving positions of the five unit cell program are at the right place (see Fig. 5).

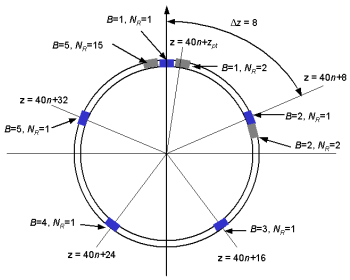

Fig. 5. Five unit cell trajectory formation using the new winding strategy.

For making a pipe several programs are necessary, once the unit cell of the fist program is established to be at the length center, the displacements Δx and the correspondent Δz displacements for each individual program are established using Eq. (3). Next the correction in z is made so as to place on the same x coordinate for all program crossing points. At this stage all unit cells have the same x coordinate, the next step is to establish the necessary Δz displacement

so as to make all unit cells from all programs coincident. Physically, this correction produces a whole pattern rotation with respect to first ply (see Fig. 6). The corrections made to the five unit cell trajectory programs are the same as those for one unit cell, but the closed trajectory condition is different see Eq. (5), also the inner cycle loop is not needed.

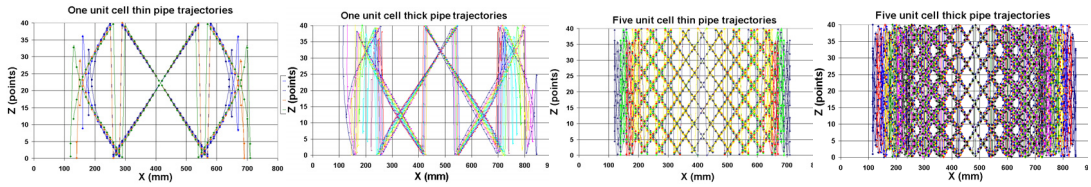

Fig. 6. One unit cell pipe trajectories (a) thin pipe trajectories, (b) thick pipe trajectories. Five unit cell pipe trajectories (c) thin pipe trajectories (d) thick pipe trajectories.

3. INSTRUMENTATION SYSTEM FOR FILAMENT WINDING SPECIMEN

A second objective was data acquisition during the different specimen fabrication phases; specimens must be instrumented with two embedded sensor types, thermocouples and optical fiber Bragg gratings, and their terminals (cables and optical fibers) must leave the mandrel by the center, (see Fig. 7).

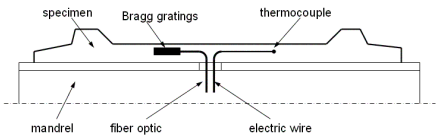

Fig. 7. Schematic embedded sensor position within the specimen.

During the curing phase the mandrel-specimen set is placed in a kind of turning spindle, (see Fig. 1c), this allows specimen rotation during oven curing. Considering all the specificities of each fabrication phase, the solution that allows sensor data acquisition during winding and curing is to direct the signal cables (optical and electrical) from the mandrel interior through the hollow machine spindle shaft.

The measuring equipment is composed of two optical fibres (each having the capacity for several Bragg gratings), and two thermocouples (4 terminals). The Bragg gratings and thermocouples being embedded, the union between the static and rotary parts is achieved by a dual fibre optic rotary joint (FORJ) and an electrical slip ring assembly. Optical lines are plugged onto the optical analyzer, and thermocouples are connected to a data acquisition card or a thermocouple temperature indicator. The system works in two possible configurations during winding and turning spindle configuration for curing. The filament winding machine uses a spindle chuck to attach the mandrel; this spindle is mounted in to a hollow shaft, providing an exit for the cables. The other mandrel side is guided by a plain center, which does not allow cable passage. This restriction leads to a coaxially mounted solution for both rotary connectors (slip ring and FORJ).

Once the specimen is polymerized, the ends must be machined off; these are not useful parts and are formed by the winding angle transition between the going and returning paths. This machining phase is needed also, because at the interface between de specimen and the hyperbaric

testing chamber there is an elastomeric joint that must be in contact over a flat surface. This machining process prevents cables and optical fibers from passing through this section.

3.1 Winding Configuration

In the winding configuration (see Fig. 8, and Table 1), the slip ring assembly (5) and the fiber optic rotary joint (6) are placed inside the mandrel, over the mandrel flask hollow shaft (1), this shaft is mounted in the mandrel flask (3) by two bearings (2) that lead a relative rotary movement between both (mandrel flask and mandrel flask hollow shaft). The mandrel flask is attached to the filament winding machine spindle chuck (14), and the mandrel flask hollow shaft is attached to the cable passage static pipe (16) by a coupling (17). This pipe is located inside the filament winding machine shaft (15) that is also a hollow shaft.

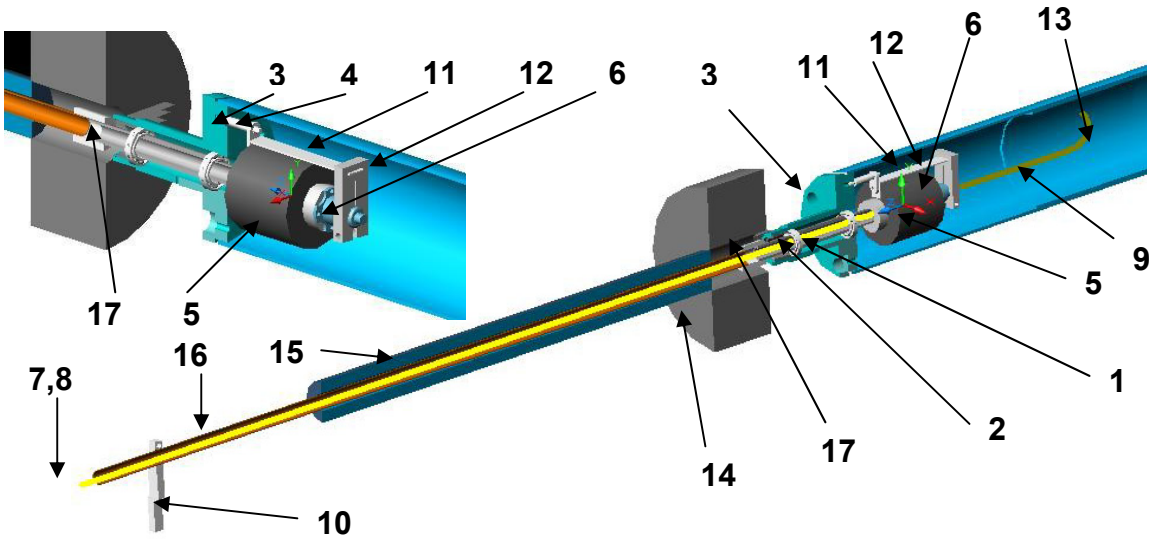

Fig. 8. Connector system and sensor cable passage in winding configuration.

Table 1. Instrumentation system part list.

No.	Item	No.	Item
1	Mandrel flask hollow shaft	10	Mandrel flask hollow shaft sychronisator
2	Bearing	11	Synchronization element
3	Mandrel Flask	12	Optical rotary joint synchronizator
4	Flask synchronizator pin	13	Mandrel
5	IEL-HS 4 terminal slip ring (2 circuits)	14	Filament winding machine spindle chuck
6	IEL-MJ2 Dual fiber optic rotary joint	15	Filament winding machine shaft
7	Static electric cables	16	Cable passage static pipe
8	Static optical fibers	17	Coupling
9	Rotary electrical and optical lines	18	Skate wheels
		19	Flask support

The cable static pipe is maintained static by the mandrel flask hollow shaft synchronizator (10) which is placed at the other end of the pipe, fixed to the filament winding machine rear cover. The cable static passage pipe exits from the winding machine cover (see Fig. 9b). The inner shaft of the slip ring assembly and one side of the fiber optic rotary joint (the one fixed to slip ring shaft) are static and the outer parts of both (slip ring and FORJ) are rotary, and are fixed to the mandrel flask by the flask synchronizator pin (4) and the synchronizator element (11). This configuration allows the outside part of slip ring and the mandrel to rotate at a same time (see Fig. 8 and 9a).

The optical and electrical lines that come from the work piece (wound pipe) (9) traverse the mandrel by a drilled hole in the middle of the mandrel (see Fig. 10), half of the hole is located on one side and the other half is located on the other mandrel half. This configuration allows mandrel extraction without optical fiber damage. The entering optical and electrical lines are connected to the outside part of the slip ring and FORJ (see Fig. 8). The cables that leave the slip ring and FORJ are directed inside the mandrel flask hollow shaft, inside the cable passage static pipe, in this way they leave the filament winding machine at the rear (see Fig. 9b).

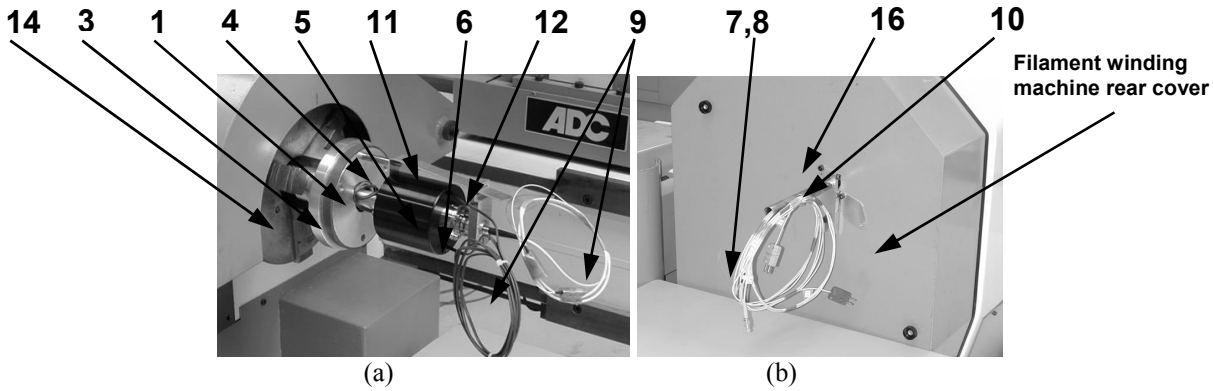

Fig. 9. Connector system in winding configuration, (a) front side view (b) rear side view.

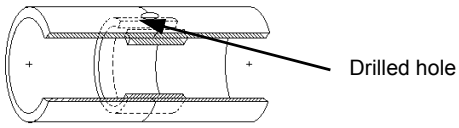

Fig. 10. Divided mandrel.

3.2 Turning spindle curing configuration

This configuration is similar to the winding one, but it does not have the cable passage static pipe, the connectors system is also located inside the mandrel, and the specimen-mandrel-connector system set is placed in a turning spindle. One mandrel flask is attached to the turning spindle header which drives the mandrel, the other mandrel side (mandrel flask) is supported by two skate wheels (18) which are placed on a plate called flask support (19), this support is attached to the turning spindle. In this configuration the mandrel flask hollow shaft synchronizer is placed directly onto the mandrel flask hollow shaft and is attached to the turning spindle structure (Fig. 11).

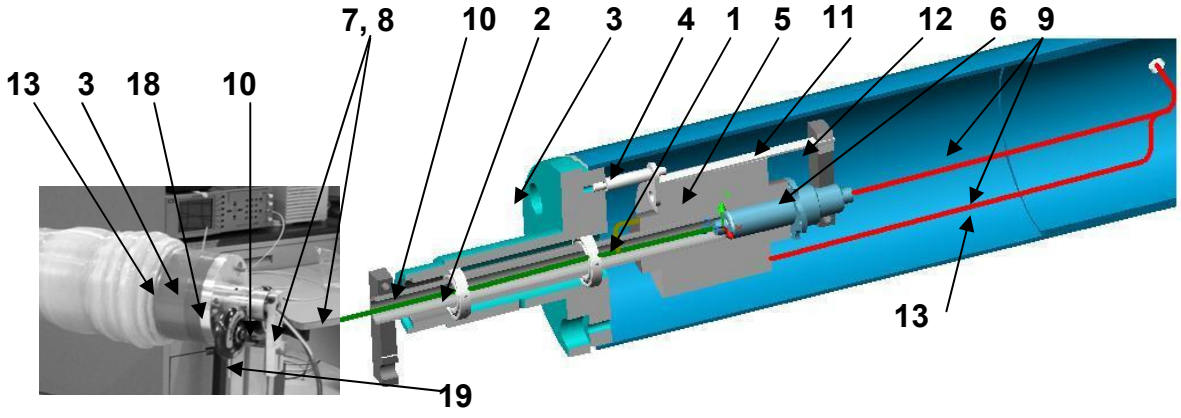

Fig.11. Connector and associated devices layout inside mandrel.

This configuration has the advantage of having the system at the mandrel interior, protecting it from possible resin spills during the fabrication process, also it offers the possibility to handle the whole system and to pass from winding configuration to turning spindle curing configuration easily.

4. RESULTS AND DISCUSSION

4.1 New programs winding tests

First winding tests have been performed with the actual roving but without resin impregnation, (dry tests), in order to confirm the validity of the programs. The test methodology used is as follows: Each program has been tested separately, first, only the going returning paths to form the first and last trajectory were wound. At this stage, the unit cells were formed. This methodology was used for all programs. Once all programs were separately tested, other series of dry tests were developed with the objective of proving the coincidence between unit cells, formed by the first trajectory of each program, and they were approved (see Fig. 12). One restriction in pipe fabrication was a constant ±55° winding angle, each consecutive program is winding over a slightly bigger diameter than the one before, in consequence the circumference

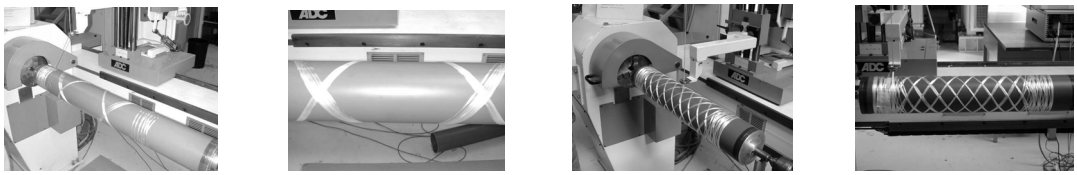

Fig. 12. Winding of all the first trajectories of each program. (a) Dry winding, (b) Program coincident unit cells, (c) Five unit cell trajectories dry winding, (d) Program coincident five unit cell trajectories.

length is also bigger, and the number of unit cells remains constant, so the unit cell size grows as well. Geometrically it is impossible to make all the unit cells exactly coincident everywhere in the pipe. Despite this fact, all unit cells are center aligned, (see Fig. 6 and 12), and all center unit cells are superposed. In the thin pipe trajectories this phenomenon is very small, but in thick pipe trajectories this is more pronounced.

Two five unit cell trajectory specimens were fabricated with the new programs. One specimen was fabricated with an embedded dummy fiber optic inside (without Bragg grating), in order to test the divided mandrel concept. The specimen was successfully extracted, without optical fiber damage (Fig. 13).

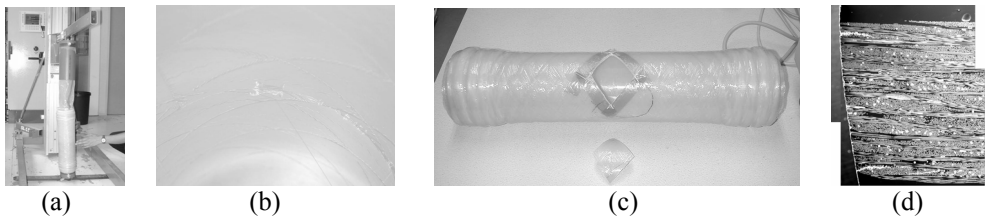

Fig. 13. a) Specimen mandrel extraction, b) Fiber optic leaving the specimen, c) Complete cell extracted from specimen, d) Micrograph showing all crossings point coincident along the thickness.

A complete unit cell was extracted from the second specimen central part. This complete unit cell was cut in slices, for proving cell alignment and to be used for future analysis (Fig. 13). One of these slices is seen in Fig. 13d, where it is shown the crossing points aligned, proving the correct programming.

4.2 Instrumentation system behavior during fabrication

An instrumented specimen was then fabricated, with a thermocouple placed beside an optical fiber with a Bragg Grating which was centered along the circumference. Both data (FBG and Thermocouple) were collected during all fabrication phases (winding, curing and mandrel extraction), proving the behavior of the connectors system (see Fig. 14).

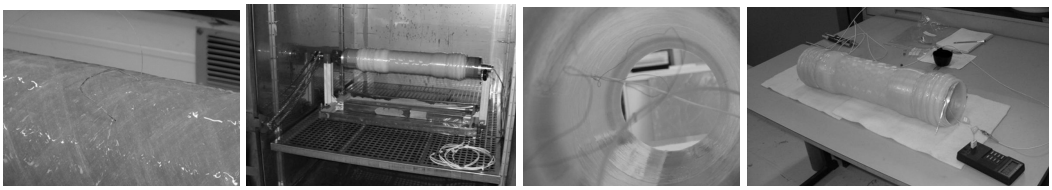

(a) (b) (c) (d)

Fig. 14. a) Optical fibre and thermocouple placing during winding, b) curing configuration, c) optical fibre and thermocouple leaving the specimen, (d) instrumented specimen.

The fabrication process is long (3 hours winding, 14 hours curing). A low frequency sampling rate has been selected (1/60 Hz), but problems were encountered in configuring the Bragg grating interrogation system, so the lowest possible frequency was chosen (5 Hz). Bragg grating data were filtered to reduce noise for obtaining useful information. Considering the large number of measurements, it was decided to record one measurement per minute, by averaging the measured values. The strain was obtained using the Eq. (6). The embedded sensors response is presented in Fig. 15a, and the resulting strain is presented in Fig. 15b.

$$\varepsilon = \frac{1}{b}\left[\frac{\Delta\lambda}{\lambda_o} - a\Delta T\right] \tag{6}$$

Where ε is the specimen strain (hoop strain), $\Delta\lambda$ is de Bragg grating wavelength shift, ΔT is the temperature variation, a is the thermo-optical coefficient ($6{,}76\text{x}10^{-6}$ 1/°C), b ($7{,}80\text{x}10^{-6}$ 1/με) is the opto-elastic coefficient and λ_0 is the characteristic Bragg grating wavelength. In Fig. 15b, it can be seen that at the end of the fabrication process, there is a residual strain of about 349 $\mu\varepsilon$. This experiment has enabled the specimen instrumentation system to be tested and its potential as a tool for a fine phenomena analysis during the fabrication process to be demonstrated.

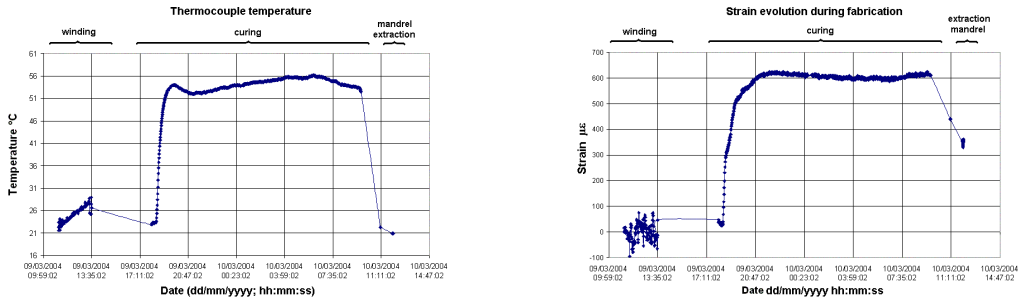

(a) (b)

Fig. 15. Evolution of embedded sensor response: (a) Temperature and (b) resulting hoop strain.

5. CONCLUSIONS

The programming for unit cell precise positioning was made, by modifying some code lines of ancient programs.

Winding programming for unit cell alignment was successfully proved.

The passage from programming to fabrication needs to be analyzed considering the specific equipment used, and the mandrel origin resetting is a key factor during fabrication.

The instrumentation system concept designed offers a solution to place the instrumentation needed for parameter evaluation during filament winding specimen fabrication.

This system has a high potential for use in detailed analysis of the fabrication of filament wound composite structures and to validate numerical modelling of filament wound tubes.

ACKNOWLEDGEMENTS

H. Hernández M. wishes to thank the National Council of Science and Technology of Mexico (CONACYT) and the National Polytechnic Institute of Mexico (IPN) for their scholarship sponsoring. The authors also thank Ivan Fernandez Hernandez and Jérémie Bauw, for their collaboration during their internship at LGMT/PRO^{2}COM.

References:

1. **Cox, B. N., Flanagan, G.**, "Handbook of Analytical Methods for Textile Composites", *NASA Contractor Report 4750*, Langley Research Center; Hampton, 1997.
2. **Hoa, S. V.,** "Analysis for Design of Fiber Reinforced Plastic Vessels and Pipings", *Technomic Publication*; Lancaster; (1991) p.1-435.
3. **Tarnpol'skii, Y. M., Kulakov, V. L., Zakrzhevskii, A. M., Mungalov; D. D.,** "Textile composite rods operating in torsion", *Compos Sci Technol*, **56**/3 (1996), 339-345.
4. **Brito, FM.,** "Influence of interwoven configuration on mechanical properties of crossed helicoidal filament winding composites", *Proc ICCM6*, (1987), 1183-89.
5. **Rousseau, J., Perreux, D., Verdière, N.,** "The influence of winding patterns on the damage behaviour of filament-wound pipes", *Compos Sci Technol*, **59** (1999), 1439-1449.
6. **Aitharaju, V. R., Averill, R.C.,** "Three – dimensional properties of woven-fabric composites"; *Compos Sci Technol*, **59** (1999), 1901-1911.
7. **Dasgupta, A., Agarwal, R.K., Bhandarkar, S.M.,** "Three-dimensional modeling of woven-fabric composites for efective thermo-mechanical and thermal properties", *Compos Sci Technol*, **56** (1996), 209-23.
8. **Byström, J., Jakabsons, N., Varna, J.,** "An evaluation of different models for prediction of elastic properties of woven composites", *Compos Part B-Eng*, **31** (2000), 7-20.
9. **Takeda, N.** "Structural Health Monitoring for Smart Composite Structure Systems in Japan"*, Ann Chim-Sci Mat*, **25** (2000), 545-549.
10. **McKenzie, I., Jones, R., I. Marshall, H., Galea, S.,** "Optical fibre sensors for health monitoring of bonded repair systems", *Compos Struct*, **50** (2000), 405-416.
11. **Okabe, Y., Mizutani, T., Yashiro, S., Takeda, N.,** "Detection of microscopic damages in composite laminates with embedded small-diameter fiber Bragg grating sensors", *Compos Sci Technol*, **62** (2002), 951-958.
12. **Degrieck, L., De Waele, W., Verleysen, P.,** "Monitoring of fibre reinforced composites with embedded optical fibre Bragg sensors, with application to filament wound pressure vessels"; *NDT&E int*; **34** (2001), 289-296.